NASA/TM-20205007448 ISABE-2019-24377

Machine Learning-Based Predictive Analytics for Aircraft Engine Conceptual Design

Michael T. Tong
Glenn Research Center, Cleveland, Ohio

October 2020

NASA STI Program . . . in Profile

Since its founding, NASA has been dedicated to the advancement of aeronautics and space science. The NASA Scientific and Technical Information (STI) Program plays a key part in helping NASA maintain this important role.

The NASA STI Program operates under the auspices of the Agency Chief Information Officer. It collects, organizes, provides for archiving, and disseminates NASA's STI. The NASA STI Program provides access to the NASA Technical Report Server—Registered (NTRS Reg) and NASA Technical Report Server—Public (NTRS) thus providing one of the largest collections of aeronautical and space science STI in the world. Results are published in both non-NASA channels and by NASA in the NASA STI Report Series, which includes the following report types:

- TECHNICAL PUBLICATION. Reports of completed research or a major significant phase of research that present the results of NASA programs and include extensive data or theoretical analysis. Includes compilations of significant scientific and technical data and information deemed to be of continuing reference value. NASA counter-part of peer-reviewed formal professional papers, but has less stringent limitations on manuscript length and extent of graphic presentations.

- TECHNICAL MEMORANDUM. Scientific and technical findings that are preliminary or of specialized interest, e.g., "quick-release" reports, working papers, and bibliographies that contain minimal annotation. Does not contain extensive analysis.

- CONTRACTOR REPORT. Scientific and technical findings by NASA-sponsored contractors and grantees.

- CONFERENCE PUBLICATION. Collected papers from scientific and technical conferences, symposia, seminars, or other meetings sponsored or co-sponsored by NASA.

- SPECIAL PUBLICATION. Scientific, technical, or historical information from NASA programs, projects, and missions, often concerned with subjects having substantial public interest.

- TECHNICAL TRANSLATION. English-language translations of foreign scientific and technical material pertinent to NASA's mission.

For more information about the NASA STI program, see the following:

- Access the NASA STI program home page at http://www.sti.nasa.gov

- E-mail your question to help@sti.nasa.gov

- Fax your question to the NASA STI Information Desk at 757-864-6500

- Telephone the NASA STI Information Desk at 757-864-9658

- Write to:
  NASA STI Program
  Mail Stop 148
  NASA Langley Research Center
  Hampton, VA 23681-2199

NASA/TM-20205007448 ISABE-2019-24377

Machine Learning-Based Predictive Analytics for Aircraft Engine Conceptual Design

Michael T. Tong
Glenn Research Center, Cleveland, Ohio

Prepared for the
24th ISABE Conference (ISABE 2019)
sponsored by the International Society for Airbreathing Engines
Canberra, Australia, September 22–27, 2019

National Aeronautics and
Space Administration

Glenn Research Center
Cleveland, Ohio 44135

October 2020

Acknowledgments

The NASA Advanced Air Transport Technology Project of the
Advanced Air Vehicles Program supports the work presented in this paper.

This work was sponsored by the Advanced Air Vehicle Program
at the NASA Glenn Research Center

Level of Review: This material has been technically reviewed by technical management.

Available from

NASA STI Program
Mail Stop 148
NASA Langley Research Center
Hampton, VA 23681-2199

National Technical Information Service
5285 Port Royal Road
Springfield, VA 22161
703-605-6000

This report is available in electronic form at http://www.sti.nasa.gov/ and http://ntrs.nasa.gov/

Machine Learning-Based Predictive Analytics for Aircraft Engine Conceptual Design

Michael T. Tong
National Aeronautics and Space Administration
Glenn Research Center
Cleveland, Ohio 44135

Abstract

Big data and artificial intelligence/machine learning are transforming the global business environment. Data is now the most valuable asset for enterprises in every industry. Companies are using data-driven insights for competitive advantage. With that, the adoption of machine learning-based data analytics is rapidly taking hold across various industries, producing autonomous systems that support human decision-making. This work explored the application of machine learning to aircraft engine conceptual design. Supervised machine-learning algorithms for regression and classification were employed to study patterns in an existing, open-source database of production and research turbofan engines, and resulting in predictive analytics for use in predicting performance of new turbofan designs. Specifically, the author developed machine learning-based analytics to predict cruise thrust specific fuel consumption (TSFC) and core sizes of high-efficiency turbofan engines, using engine design parameters as the input. The predictive analytics were trained and deployed in Keras, an open-source neural networks application program interface (API) written in Python, with Google's TensorFlow (an open source library for numerical computation) serving as the backend engine. The promising results of the predictive analytics show that machine-learning techniques merit further exploration for application in aircraft engine conceptual design.

Nomenclature

API	application program interface
BPR	bypass ratio
ANN	Artificial Neural Networks
DNN	Deep Neural Networks
HPC	high-pressure compressor
h	HPC last-stage blade height (core size)
OPR	overall pressure ratio
SVM	Support Vector Machine
TSFC	thrust specific fuel consumption
C	SVM parameter, controls the tradeoff between misclassification error and separation margin
Υ	SVM parameter, controls the tradeoff between error due to bias and variance in the model
N_h	number of hidden layers
N_e	number of neurons in each hidden layer

1.0 Introduction

The aviation industry is capital intensive, and is subject to stringent environmental and safety regulations. To minimize risk, technological improvements of aircraft engines are generally made incrementally, drawing heavily from experiences and lessons learned. Engine companies have generated and collected large amounts of data over the years. These big data, from various sources such as the database of currently manufactured engines, current development projects, previously completed development projects, and the designs that were not manufactured, are valuable resources of intelligence that can support new engine development. With increasing computational power and employing machine learning, data can be mined to provide valuable insights that could bring high levels of efficiency to engine conceptual design.

The author's previous study (Ref. 1) showed that machine learning-based analytics could be an effective tool for turbofan core-size prediction. In this work, the focus was on the application of machine-learning analytics for turbofan TSFC prediction. Supervised machine-learning algorithms for regression were employed to find patterns in the database of 183 manufactured engines and engines that were studied previously in various NASA aeronautics projects. Analytics for turbofan cruise TSFC prediction was built. The objective was to determine if machine learning-based predictive analytics could be an effective tool for turbofan engine TSFC prediction at the conceptual design stage. In addition to the TSFC predictive-analytics development, the author slightly modified the engine core-size predictive analytics that was developed in Reference 1, to improve its prediction accuracy. The modification accounted for an additional (the fourth) input parameter, *engine technology level*.

Both TSFC and core-size are key design parameters for any new aircraft engine. TSFC is a measure of fuel efficiency. It affects aircraft range and is a key element in fuel burn. TSFC is also an indicator of engine operating cost. To be able to predict TSFC rapidly and accurately would help to identify the best engine design expeditiously amongst several candidates. Engine core size can affect fuel efficiency. To be able to predict engine core size rapidly and accurately in the design space exploration would facilitate engine core architecture selection in the conceptual stage of engine development.

2.0 Engine Database

The basic engine architecture in this study was an axial-compressor turbofan. The engine database consisted of 144 manufactured engines (Refs. 2 to 8) and 39 engines that were studied previously in various NASA aeronautics projects. These commercial engines span the era from the mid-1960s to mid-2010s. The database captures over half-a-century of engine technology improvements and lessons-learned, which injects realism to the predictive analytics. The NASA engine data were the system-study results for various NASA aeronautics projects (Refs. 9 to 15). The engine database is shown in the Appendix (Table IX).

3.0 Machine Learning Algorithms

Machine learning is a branch of artificial intelligence that uses statistical technique and mathematical algorithms to enable a machine to learn from data, to analyze data patterns, and to make decisions with minimal human intervention. In this work, the author developed a machine learning-based predictive analytics for TSFC predictions.

For engine core-size prediction the support vector machine algorithm (SVM) was used. In a previous study (Ref. 1), of the three algorithms studied, SVM offered the best accuracy and the lowest uncertainty for binary classification.

3.1 Support Vector Machine (SVM) for Engine Core-Size Classification

In this work, engine core-size prediction was treated as a classification problem, since the actual engine core sizes for the commercial engines were not publicly available. A machine-learning predictive analytics based on SVM (Ref. 16), which was developed in previous study (Ref. 1), was slightly modified for engine core-size classification, i.e. to label engine core size as *acceptable* or *unacceptable.* The modification accounted for an additional (the fourth) input parameter, *engine technology level*, as described in the next section. The algorithm is also described in Reference 1.

3.2 Deep Neural Network (DNN) for Cruise TSFC Regression

Cruise TSFC prediction was considered a regression problem. Due to the high degree of accuracy required for the TSFC prediction, its predictive analytics was developed using a deep-learning neural network (DNN) that established correlations between the input variables and the TSFC. DNN is essentially an artificial neural network (Ref. 17) with several hidden layers. In this work, the DNN consisted of one input layer, six hidden layers, and one output layer. Each subsequent hidden layer, consisted of six neurons, progressively extracting higher-level features from the input. These layers used backpropagation to optimize the weights of the input variables to improve the predictive power of the analytics. A scaled exponential linear unit (SELU) function (Ref. 18) was used for the activation function in the hidden layers, defined as:

$$SELU(x) = scale \begin{cases} x & if\ x > 0 \\ \alpha e^{x} - \alpha & if\ x \leq 0 \end{cases}$$

where x = weighted sum of input variables

$\alpha \approx 1.67326$, a predefined constant to preserve the mean and variance of the inputs

$scale \approx 1.05070$, a predefined constant to preserve the mean and variance of the inputs

Dropout regularization technique (Ref. 19), where neuron outputs are dropped out randomly, was applied between the fifth and the sixth hidden layers, and between the sixth hidden layer and the output layer, to prevent the DNN from overfitting the training data. The dropout rate was set to 20 percent. A grid-search routine was used to determine number of epochs, batch size that give the lowest training error. The number of epochs determined the number of times an entire training dataset was passed forward and backward through the DNN. Batch size referred to the number of training samples used for each iteration. The Adam optimization algorithm (Ref. 20) was used for this effort. The predictive analytics was trained and deployed in Keras (Ref. 18), an open-source neural networks API written in Python, with Google's TensorFlow (Ref. 21) serving as the backend engine. Keras provided the building blocks for developing the deep-learning analytics, and TensorFlow handled the tensor computations and manipulations. TensorFlow is an open source library for numerical computation and large-scale machine learning.

4.0 Predictive Analytics

With the machine learning algorithms described in the previous section, the author developed two types of predictive analytics: a regression model for turbofan cruise TSFC prediction, and a classification model for turbofan core-size prediction. Similar to Reference 1, core sizes of all the manufactured engines are assumed to be 0.5 in. or larger. For the NASA engines, core sizes were classified according to the blade-height data obtained from the system studies. The Python programming language (script and libraries) was used to develop both analytics.

Input engine parameters for cruise TSFC predictive analytics were:

- OPR at sea level static condition
- BPR at sea level static condition
- Sea level static thrust
- Cruise Mach number
- Cruise altitude
- Engine technology level (engine certified year)

Even though turbine inlet temperature (T4), turbine cooling, and turbomachinery efficiencies were important design parameters, these engine data were not publicly available. However, their high dependence on engine technology (such as tip-clearance control and advanced materials) are well understood. Since in general, "*engine certified year*" is a good indicator of engine technology level, it was used to account for T4, turbine cooling, and turbomachinery efficiencies. For the NASA engines, the certification years were assumed to be 2025, 2030, and 2040 respectively to correspond with the N+1, N+2, and N+3 timeframes. These timeframes were directed at three generations of aircraft in the near, mid, and far terms that were studied under NASA aeronautics projects. The sea-level flight condition for OPR and BPR was chosen for data availability; majority design data for these two parameters are publicly available at the sea-level flight condition.

For engine core-size predictive analytics, the binary classifier that was developed in Reference 1 was slightly modified to account for an additional (the fourth) input parameter, *engine technology level*.

Input engine parameters for core-size predictive analytics were:

- OPR at sea level static condition
- BPR at sea level static condition
- Sea level static thrust
- Engine technology level (engine certified year)

Two predictive analytics were built with the machine-learning algorithms described in the previous section. The predictive analytics for cruise TSFC was a regression model. The predictive analytics for engine core-size was a binary classifier. The core sizes were categorized into two classes: 0 and 1 (correspond to *acceptable* and *unacceptable* core sizes), according to the engine core size (h), as shown in Table I.

TABLE I.—CATEGORIES OF ENGINE CORE-SIZE CLASSIFIER

Two classes	
0 (acceptable)	1 (unacceptable)
$h \geq 0.50$ in.	$h < 0.50$ in.

TABLE II.—TRAINING-TESTING DATASET SPLIT FOR THE PREDICTIVE ANALYTICS

Training dataset (no. of engines)	Testing dataset (no. of engines)
137 (75% of dataset)	46 (25% of dataset)

Training and building the predictive analytics involved machine learning algorithms and data science. The approach consisted of three steps: dataset preparation; building, training, and cross-validation of the preliminary analytics; and building, training, and evaluation of the final analytics.

- Dataset preparation

The engine dataset was shuffled randomly (using pseudo-random number generator) and divided into two datasets: the training set and the testing set. The training set was used to train, cross-validate, and build predictive analytics. The testing set consisted of the remaining engines that were unseen by the predictive analytics, and was retained for the final evaluation of the predictive analytics. Table II depicts the training-testing dataset split.

- Building, training, and cross-validation of the preliminary analytics

The building, training and cross-validation of the analytics were conducted using the training dataset. Within the training dataset (137 engines), a 6-fold cross-validation procedure was used to conduct a preliminary evaluation and to fine-tune the analytics. The training dataset was randomly split into 6 groups: 5 groups were used to train the analytics and 1 group was used to cross-validate the analytics. This process was repeated 6 times so that each of the 6 groups got the chance to be used for training and validation. The performance measure was then the average of the values, in terms of the mean and standard deviation, computed in the iteration loop.

- Building, training, and evaluation of the final analytics

Cross-validation was no longer needed for this step, i.e., all 137 engine data were used to build and train the predictive analytics. The analytics were then used to predict the cruise TSFC and core sizes in the testing dataset (46 engines), and the results were compared with the testing dataset.

5.0 Predictive Results

5.1 Preliminary Training and Cross-Validation Results

During preliminary training and cross validation, the algorithm parameters and prediction uncertainties were determined. Using grid-search routines, the algorithms parameters that give the smallest errors for both analytics are shown in Table III.

TABLE III.—ALGORITHMS USED AND THEIR PARAMETERS

Algorithms	Parameters
DNN for TSFC prediction	N_h = 6, N_e = 6, epoch=8386, batch size = 16, dropout rate for the 5th and 6th hidden layers = 20%
SVM for core-size prediction	C = 10, Υ = 1

TABLE IV.—CROSS-VALIDATION RESULTS

Algorithms	Accuracy (average)	Uncertainty 95% confidence interval (two standard deviations)
DNN for cruise TSFC prediction	97.9%	3.5%
SVM for core-size prediction	97.8%	4.3%

The prediction accuracy for TSFC measured how close the prediction was to the test data. The uncertainty was defined at 95 percent confidence level, i.e., two standard deviations for normal data distribution. The cross validation results are shown in Table IV. For the core-size prediction, the classification accuracy of the algorithms was defined as the number of correct predictions made as a percentage of all predictions made. Its uncertainty was also defined at 95 percent confidence interval. The results show close to 98 percent prediction accuracy for both TSFC and core sizes, with 3.5 and 4.3 percent uncertainties, respectively.

5.2 Evaluation of the Final Predictive Analytics With Testing Dataset

5.2.1 TSFC Prediction

The final predictive analytics, built with the parameters determined during the preliminary training and with all 137 training data (i.e., no cross validation), were then used to predict the engine TSFC and core sizes in the testing dataset (the 46 engines unseen by the analytics). Table V summarizes the evaluation results of the TSFC predictive analytics. On average, the prediction accuracy is high, at 98.3 percent. Table VI shows the detailed comparison of the prediction and the testing data. The prediction accuracy exceeds 95 percent for 45 of the 46 engines. The prediction accuracy for the one engine is only slightly below 95 percent. The performance of the deep-learning model over time during training is shown in Figure 1. It shows the mean squared error decreases consistently and converges over training epochs. The DNN model performs well consistently for both the training and testing datasets. An epoch is a measure of the number of times an entire dataset is passed forward and backward through the neural network.

TABLE V.—EVALUATION RESULTS OF THE CRUISE TSFC PREDICTIVE ANALYTICS

Accuracy (average)	Accuracy (maximum)	Accuracy (minimum)
98.3%	100.0%	94.8%

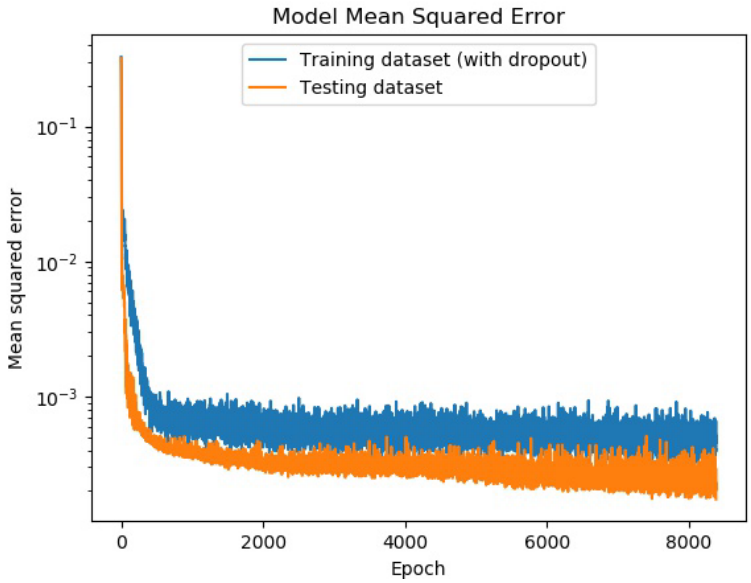

Figure 1.—Deep Neural Network model accuracy on training and testing datasets.

TABLE VI.—COMPARISON OF TSFC PREDICTIONS WITH TESTING DATASET

Org.	Engine model	Cruise TSFC Data	Cruise TSFC Prediction	Accuracy, %	Org.	Engine model	Cruise TSFC Data	Cruise TSFC Prediction	Accuracy, %
P&W	4056	0.560	0.581	96.3	NASA ERA	Large-Geared-2015-HWB-V2	0.464	0.466	99.6
CFM	56-5A5	0.596	0.583	97.8	GE	CF6-80C2A3	0.576	0.581	99.1
GE	CF6-80E1A1	0.562	0.576	97.5	NASA ERA	Small-Geared-2015	0.485	0.485	100.0
GE	CF6-80E1A3	0.562	0.569	98.8	NASA SFW	Simulated GE90-110B	0.549	0.531	96.7
Rolls Royce	Trent 1000-A	0.506	0.513	98.6	GE	CF34-3A	0.704	0.717	98.2
CFM	LEAP-1A35	0.536	0.527	98.3	P&W	1519G	0.544	0.530	97.4
Rolls Royce	Trent 890-17	0.560	0.561	99.8	GE	CF6-80C2B2	0.576	0.580	99.3
GE	90-94B	0.545	0.546	99.8	P&W	JT9D-20	0.624	0.622	99.7
Rolls Royce	BR715-A1-30	0.620	0.612	98.7	P&W	JT8D-17R	0.825	0.789	95.6
P&W	4074	0.560	0.549	98.0	P&W	4060	0.560	0.578	96.8
GE	CF6-6D	0.646	0.638	98.8	P&W	4460	0.560	0.574	97.5
NASA SFW	SA-FPR1.5-GR-HW-2E	0.515	0.512	99.4	NASA ERA	Large-Geared-2014	0.458	0.458	100.0
NASA SFW	SA-FPR1.3-GR-HW-2D	0.470	0.480	97.9	CFM	CFM56-5B1	0.600	0.577	96.2
P&W	JT9D-7Q	0.631	0.627	99.4	P&W	2040	0.563	0.579	97.2
NASA ERA	Small-Geared-2014	0.486	0.478	98.4	GE	CF6-50C1	0.657	0.649	98.8
GE	CF34-8C1	0.664	0.683	97.1	P&W	JT9D-7J	0.631	0.630	99.8
CFM	56-5A4	0.596	0.593	99.5	NASA SFW	SA-FPR1.5-GR-HW-2D	0.502	0.501	99.8
P&W	4090	0.560	0.553	98.8	P&W	2037	0.563	0.592	94.8 ⬅
P&W	JT9D-7A	0.625	0.623	99.7	GE	90-76B	0.545	0.548	99.4
Rolls Royce	BR715-C1-30	0.620	0.588	94.8	NASA SFW	SA-FPR1.4-DD-2D	0.479	0.490	97.7
NASA ERA	Small-DD-2015-V2	0.524	0.511	97.5	Rolls-Royce	Trent 875	0.560	0.560	100.0
P&W	JT9D-7R4H1	0.628	0.610	97.1	CFM	56-2C1	0.651	0.665	97.8
GE	GEnx-1B64	0.514	0.518	99.2	GE	CF6-50C	0.657	0.648	98.6

Average accuracy = 98.3 percent ⬅ lowest accuracy

SFW – Subsonic Fixed Wing project
ERA – Environmentally Responsible Aviation project

5.2.2 Core-Size Prediction

Table VII shows the evaluation results of the core-size predictive analytics. The analytics performs remarkably; it has a perfect prediction accuracy. More importantly, it also predicts unacceptable engine core sizes ($h < 0.5$ in.) with perfect accuracy. Table VIII shows the detailed comparison of the prediction and the testing data.

TABLE VII.—EVALUATION RESULTS OF THE ENGINE CORE-SIZE PREDICTIVE ANALYTICS

Core size	No. of engines (data)	No. of engines (predictions)	Accuracy
$h \geq 0.5$ in.	40	40	100%
$h < 0.5$ in.	6	6	100%
Overall	46	46	100%

TABLE VIII.—COMPARISON OF ENGINE CORE-SIZE PREDICTIONS WITH TESTING DATASET

Org.	Engine model	Core size Data	Core size Prediction	Org.	Engine model	Core size Data	Core size Prediction
P&W	2043	●	●	NASA SFW	SA-FPR1.6-GR-HW-2E	▲	▲
IAE	V2525-D5	●	●	NASA SFW	Simulated Genx	●	●
IAE	V2533-A5	●	●	Rolls Royce	RB211-524B4-02	●	●
CFM Int'l	56-5B2	●	●	IAE	V2522-A5	●	●
GE	90-76B	●	●	CFM Int'l	56-5C3	●	●
IAE	V2500-A1	●	●	IAE	V2530-A5	●	●
P&W	JT9D-20	●	●	Rolls Royce	RB211-535E4	●	●
Rolls Royce	Trent 970-84	●	●	Rolls Royce	Trent XWB-97	●	●
P&W	JT9D-7R4H1	●	●	NASA SFW	SA-FPR1.4-GR-HW-2E	▲	▲
NASA SFW	SA-FPR1.5-GR-HW-2E	▲	▲	CFM Int'l	CFM56-5B6/P	●	●
NASA AATT	N3CC-2018	▲	▲	NASA ERA	Large-DD-2015	●	●
Rolls Royce	RB211-22B	●	●	P&W	JT9D-7R4G2	●	●
CFM Int'l	CFM56-7B22	●	●	P&W	PW4090	●	●
Rolls Royce	Trent 772	●	●	NASA ERA	Small-Geared-2015	▲	▲
GE	CF34-8E5A2	●	●	Rolls Royce	RB211-524C2	●	●
GE	GE90-85B	●	●	P&W	4462	●	●
GE	CF6-80E1A4	●	●	P&W	4460	●	●
P&W	PW4056	●	●	NASA SFW	SA-FPR1.4-DD-2D	▲	▲
GE	CF6-80C2B4	●	●	CFM Int'l	56-5C2	●	●
P&W	JT9D-7R4D	●	●	P&W	4056	●	●
GE	CF6-80E1A2	●	●	GE	GEnx-1B58	●	●
P&W	PW4052	●	●	Rolls Royce	RB211-524B	●	●
P&W	PW4164	●	●	P&W	JT8D-17AR	●	●

● $h \geq 0.50$ in. ▲ $h < 0.50$ in.

SFW – Subsonic Fixed Wing project
ERA – Environmentally Responsible Aviation project
AATT – Advanced Air Transport Technology project

6.0 Conclusions

The author developed two machine-learning predictive analytics for turbofan TSFC and core-size predictions, respectively. The development used the database of 183 manufactured engines and engines that were studied previously in NASA aeronautics projects. The TSFC predictive analytics has an average accuracy of 98.3 percent, with 3.5 percent uncertainty. The engine core-size predictive analytics has an overall accuracy of 100 percent, with 4.3 percent uncertainty. Overall, both predictive analytics show remarkable prediction accuracy.

To further improve the accuracy (and reduce the uncertainty) of TSFC prediction, the database needs to be expanded. However, the limitation of publicly available engine data is a challenge to overcome. Overall, the results show that by bringing together sufficient (big) high quality data, robust machine-learning algorithms, and data science, machine learning-based predictive analytics can be an effective tool for engine design-space exploration during the conceptual design phase. It would help to identify the best engine design expeditiously amongst several candidates. The promising results of the predictive analytics show that machine-learning techniques merit further exploration for application in aircraft engine conceptual design.

References

1. Tong, M.T., "Using Machine Learning To Predict Core Sizes of High-Efficiency Turbofan Engines," GT2019-91432, ASME Turbo-Expo 2019, June 17-21, 2019.
2. Daly, M., "Jane's Aero-Engine," 2017-2018.
3. Meier, N., "Civil turbojet/turbofan specifications." http://www.jet-engine.net/civtfspec.html. Accessed August, 2018.
4. GE Aviation. https://www.geaviation.com/commercial
5. Pratt and Whitney. https://www.pw.utc.com/products-and-services/products/commercial-engines
6. Rolls Royce. https://www.rolls-royce.com/products-and-services/civil-aerospace
7. CFM International. https://www.cfmaeroengines.com/
8. International Civil Aviation Organization, "ICAO Aircraft Emissions Databank." May, 2018.
9. Guynn, M.D., Berton, J.J., Fisher, K.L., Haller, W.J., Tong, M., Thurman, D.R., "Engine Conceptual Study for an Advanced Single-Aisle Transport," NASA/TM—2009-215784, August 2009.
10. Guynn, M.D., Berton, J.J., Fisher, K.L., Haller, W.J., Tong, M., Thurman, D.R., "Analysis of Turbofan Design Options for an Advanced Single-Aisle Transport Aircraft," AIAA 2009-6942, September 2009.
11. Guynn, M. D., Berton, J.J., Fisher, K.L., Haller, W.J., Tong, M., Thurman, D.R, "Refined Exploration of Turbofan Design Options for an Advanced Single-Aisle Transport," NASA/TM—2011-216883, January 2011.
12. Guynn, M.D., Berton, J.J., Tong, M.T., Haller, W.J., "Advanced Single-Aisle Transport Propulsion Design Options Revisited," AIAA 2013-4330, August 2013.
13. Nickol, C.L. and Haller W.J., "Assessment of the Performance Potential of Advanced Subsonic Transport Concepts for NASA's Environmentally Responsible Aviation Project," AIAA 2016-1030, January 2016.
14. Collier, F., Thomas, R., Burley, C., Nickol, C., Lee, C.M., Tong, M., "Environmentally Responsible Aviation – Real Solutions for Environmental Challenges Facing Aviation," 27th International Congress of the Aeronautical Sciences, September, 2010.
15. Jones, S.M., Haller, W.J., Tong, M.T., "An N+3 Technology Level Reference Propulsion System," NASA/TM—2017-219501, May, 2017.

16. Ng, A., “Support Vector Machines.” CS229 lecture notes. Stanford University. http://cs229.stanford.edu/notes/cs229-notes3.pdf
17. Ng, A., “Machine Learning,” Coursera online course lecture notes. https://www.coursera.org/learn/machine-learning
18. Chollet, François and others, “Keras.” Retrieved on February 22, 2019 from: https://keras.io/
19. Hinton, G.E., Krizhevsky, A., Srivastava, N., Sutskever, I., & Salakhutdinov, R., “Dropout: A simple Way to Prevent Neural Networks from Overfitting.” Journal of Machine Learning Research, 15, 1929-1958. June, 2014.
20. Kingma, D. P. and Ba, J., “Adam: A Method for Stochastic Optimization,” International Conference on Learning Representations, May 2015.
21. Google, “TensorFlow: Large-Scale Machine Learning on Heterogeneous Distributed Systems. Retrieved on February 20, 2019 from: https://www.tensorflow.org/

Appendix. Engine Database

TABLE IX.—ENGINE DATABASE

Org.	Engine Model	BPR (SLS)	OPR (SLS)	Thrust, lbs (SLS)	Cruise Mach	Cruise Alt. k ft.	Year certified	Cruise TSFC lb/lbf.hr	Core Size
CFM Int'l	CFM56-2C1	6.0	23.50	22000	0.80	35	1979	0.651	●
CFM Int'l	CFM56-3B1	5.1	22.40	20000	0.80	35	1984	0.655	●
CFM Int'l	CFM56-3B2	5.1	24.30	22000	0.80	35	1984	0.655	●
CFM Int'l	CFM56-3C1	5.1	25.50	23500	0.80	35	1986	0.667	●
CFM Int'l	CFM56-5A1	6.0	26.60	25000	0.80	35	1987	0.596	●
CFM Int'l	CFM56-5A3	6.0	27.90	26500	0.80	35	1990	0.596	●
CFM Int'l	CFM56-5A4	6.0	23.80	22000	0.80	35	1996	0.596	●
CFM Int'l	CFM56-5A5	6.0	25.10	23500	0.80	35	1996	0.596	●
CFM Int'l	CFM56-5B1	5.7	30.20	30000	0.80	35	1994	0.600	●
CFM Int'l	CFM56-5B2	5.6	31.30	31000	0.80	35	1993	0.600	●
CFM Int'l	CFM56-5B3	5.4	32.60	33300	0.80	35	1997	0.600	●
CFM Int'l	CFM56-5B4	5.9	27.10	27000	0.80	35	1994	0.600	●
CFM Int'l	CFM56-5B5/P	5.9	23.33	22000	0.80	35	1996	0.600	●
CFM Int'l	CFM56-5B6/P	6.0	24.64	23500	0.80	35	1995	0.600	●
CFM Int'l	CFM56-5C2	6.8	28.80	31200	0.80	35	1991	0.545	●
CFM Int'l	CFM56-5C3	6.7	29.90	32500	0.80	35	1994	0.567	●
CFM Int'l	CFM56-5C4	6.6	31.15	34000	0.80	35	1994	0.567	●
CFM Int'l	CFM56-7B20	5.4	22.61	20600	0.80	35	1996	0.603	●
CFM Int'l	CFM56-7B22	5.3	24.41	22700	0.80	35	1996	0.603	●
CFM Int'l	CFM56-7B24	5.2	25.78	24200	0.80	35	1996	0.603	●
CFM Int'l	CFM56-7B26	5.1	27.61	26300	0.80	35	1996	0.603	●
CFM Int'l	CFM56-7B27	5.0	28.63	27300	0.80	35	1996	0.603	●
CFM Int'l	LEAP-1A26	11.1	33.40	27112	0.78	35	2015	0.536	●
CFM Int'l	LEAP-1A35	10.7	38.60	32170	0.78	35	2015	0.536	●
CFM Int'l	LEAP-1B25	8.4	38.40	26797	0.79	35	2016	0.536	●
CFM Int'l	LEAP-1B27	8.5	39.90	28034	0.79	35	2016	0.536	●
CFM Int'l	LEAP-1B28	8.6	41.50	29315	0.79	35	2016	0.536	●
GE	CF6-6D	5.9	24.70	40000	0.85	35	1970	0.646	●
GE	CF6-6D1	5.9	24.70	41500	0.85	35	1971	0.646	●
GE	CF6-6D1A	5.9	25.40	41500	0.85	35	1971	0.646	●
GE	CF6-45A2	4.3	25.90	46500	0.85	35	1973	0.630	●
GE	CF6-50C	4.3	28.80	51000	0.85	35	1975	0.657	●
GE	CF6-50C1	4.3	29.80	52500	0.85	35	1975	0.657	●
GE	CF6-50C2	4.3	28.44	52500	0.85	35	1978	0.630	●
GE	CF6-50C2B	4.3	29.06	54000	0.85	35	1979	0.630	●
GE	CF6-50E	4.3	28.44	52500	0.85	35	1973	0.657	●
GE	CF6-50E2	4.3	29.80	52500	0.85	35	1973	0.630	●
GE	CF6-80A	5.0	29.00	48000	0.80	35	1981	0.623	●
GE	CF6-80A2	5.0	30.10	50000	0.80	35	1981	0.623	●
GE	CF6-80A3	5.0	30.10	50000	0.80	35	1981	0.623	●
GE	CF6-80C2A1	5.1	30.96	59000	0.80	35	1985	0.576	●
GE	CF6-80C2A2	5.1	28.00	52460	0.80	35	1986	0.578	●
GE	CF6-80C2A3	5.1	31.64	58950	0.80	35	1988	0.576	●
GE	CF6-80C2A5	5.1	31.58	60100	0.80	35	1988	0.578	●
GE	CF6-80C2A8	5.1	31.00	59000	0.80	35	1996	0.602	●
GE	CF6-80C2B1	5.1	30.08	56700	0.80	35	1987	0.576	●
GE	CF6-80C2B1F	5.1	30.13	57160	0.80	35	1989	0.564	●
GE	CF6-80C2B2	5.1	27.74	51590	0.80	35	1987	0.576	●
GE	CF6-80C2B4	5.1	30.36	57180	0.80	35	1987	0.590	●
GE	CF6-80C2B6	5.1	31.56	60070	0.80	35	1987	0.602	●
GE	CF6-80E1A1	5.1	32.46	67500	0.80	35	1993	0.562	●
GE	CF6-80E1A2	5.1	33.10	68240	0.80	35	1993	0.562	●
GE	CF6-80E1A3	5.1	35.70	68520	0.80	35	2001	0.562	●
GE	CF6-80E1A4	5.1	34.50	66870	0.80	35	1997	0.562	●
GE	CF34-10A	5.4	26.50	18290	0.74	37	2010	0.650	●
GE	CF34-10E	5.1	27.30	18820	0.74	37	2002	0.665	●
GE	CF34-3A	6.3	19.70	9220	0.74	37	1986	0.704	●
GE	CF34-8C1	5.1	23.03	12670	0.74	37	1999	0.664	●
GE	CF34-8C5	5.1	23.09	13358	0.74	37	2002	0.680	●
GE	CF34-8E5A2	5.1	24.82	14500	0.74	37	2002	0.680	●
GE	GE90-76B	8.6	35.45	79654	0.80	35	1995	0.545	●

● $h \geq 0.50$ in.

SFW – Subsonic Fixed Wing project
ERA – Environmentally Responsible Aviation project
AATT – Advanced Air Transport Technology project

TABLE IX.—Continued.

Org.	Engine Model	BPR (SLS)	OPR (SLS)	Thrust, lbs (SLS)	Cruise Mach	Cruise Alt. k ft.	Year certified	Cruise TSFC lb/lbf.hr	Core Size
GE	GE90-85B	8.4	38.37	87315	0.80	35	1995	0.553	●
GE	GE90-90B	8.4	39.70	94000	0.80	35	1997	0.545	●
GE	GE90-94B	8.3	40.53	97300	0.80	35	2000	0.545	●
GE	GE90-115B	7.1	42.24	115529	0.80	35	2003	0.550	●
GE	GEnx-1B54	9.4	35.20	57394	0.85	40	2008	0.514	●
GE	GEnx-1B58	9.2	37.20	60991	0.85	40	2008	0.514	●
GE	GEnx-1B64	9.0	40.60	66993	0.85	40	2008	0.514	●
GE	GEnx-1B70	8.8	43.50	72299	0.85	40	2008	0.514	●
P&W	JT8D-7	1.1	15.82	14000	0.80	35	1966	0.796	●
P&W	JT8D-9	1.0	15.88	14500	0.80	35	1967	0.807	●
P&W	JT8D-17AR	1.0	17.28	16400	0.80	35	1982	0.825	●
P&W	JT8D-17R	1.0	18.24	17400	0.80	35	1976	0.825	●
P&W	JT8D-209	1.8	18.30	18500	0.80	35	1979	0.724	●
P&W	JT8D-219	1.7	20.27	21000	0.80	35	1985	0.737	●
P&W	JT9D-3A	5.2	21.50	44300	0.85	35	1969	0.624	●
P&W	JT9D-7	5.2	22.20	46300	0.85	35	1971	0.620	●
P&W	JT9D-7A	5.1	20.30	46950	0.85	35	1972	0.625	●
P&W	JT9D-7F	5.1	22.80	48000	0.85	35	1974	0.631	●
P&W	JT9D-7J	5.1	23.50	50000	0.85	35	1976	0.631	●
P&W	JT9D-7Q	4.9	24.50	53000	0.85	35	1978	0.631	●
P&W	JT9D-7R4D	5.0	23.40	48000	0.85	35	1978	0.615	●
P&W	JT9D-7R4E	5.0	24.20	50000	0.85	35	1982	0.620	●
P&W	JT9D-7R4G2	4.8	26.30	54750	0.85	35	1982	0.639	●
P&W	JT9D-7R4H1	4.8	26.70	56000	0.85	35	1982	0.628	●
P&W	JT9D-20	5.2	20.30	46300	0.85	35	1972	0.624	●
P&W	JT9D-70A	4.9	24.50	53000	0.85	35	1974	0.631	●
P&W	1127G	12.3	31.70	27000	0.78	35	2014	0.530	●
P&W	1519G	11.6	32.30	19000	0.78	35	2013	0.544	●
P&W	2037	6.0	26.90	37600	0.80	35	1983	0.563	●
P&W	2040	5.5	29.40	40900	0.80	35	1987	0.563	●
P&W	2043	5.3	31.90	42600	0.80	35	1995	0.563	●
P&W	4052	5.0	26.32	52200	0.85	35	1987	0.560	●
P&W	4056	4.7	29.30	56750	0.85	35	1986	0.560	●
P&W	4060	4.5	32.40	60000	0.85	35	1988	0.560	●
P&W	4074	6.8	32.20	74500	0.85	35	1994	0.560	●
P&W	4077	6.7	33.20	77000	0.85	35	1994	0.560	●
P&W	4084	6.4	36.20	84000	0.85	35	1994	0.560	●
P&W	4090	6.1	39.16	90200	0.85	35	1996	0.560	●
P&W	4098	5.8	41.37	95340	0.85	35	1998	0.560	●
P&W	4152	4.9	26.90	52200	0.85	35	1986	0.560	●
P&W	4156	4.7	29.30	56750	0.85	35	1986	0.560	●
P&W	4164	5.2	31.24	64000	0.85	35	1993	0.560	●
P&W	4168-1D	4.9	33.10	68600	0.85	35	2008	0.560	●
P&W	4460	4.7	30.68	60000	0.85	35	1988	0.560	●
P&W	4462	4.6	31.91	63300	0.85	35	1992	0.560	●
P&W	6122A	4.8	25.70	22100	0.80	35	2004	0.540	●
Rolls-Royce	RB211-22B	4.7	25.00	41000	0.85	35	1973	0.655	●
Rolls-Royce	RB211-524B	4.5	28.40	49100	0.85	35	1973	0.633	●
Rolls-Royce	RB211-524B4-02	4.4	29.00	50000	0.85	35	1981	0.603	●
Rolls-Royce	RB211-524C2	4.5	29.10	51500	0.85	35	1979	0.656	●
Rolls-Royce	RB211-524D4	4.3	29.70	53000	0.85	35	1983	0.631	●
Rolls-Royce	RB211-524G	4.3	32.10	58000	0.85	35	1989	0.582	●
Rolls-Royce	RB211-524H	4.2	34.00	60600	0.85	35	1989	0.572	●
Rolls-Royce	RB211-535C	4.5	21.50	37400	0.80	35	1981	0.646	●
Rolls-Royce	RB211-535E4	4.1	25.40	40100	0.80	35	1983	0.598	●
Rolls-Royce	AE3007A	5.2	18.08	7580	0.78	32	1997	0.625	●
Rolls-Royce	BR710-A1-10	4.2	24.23	14750	0.80	35	1996	0.630	●
Rolls-Royce	BR715-A1-30	4.7	28.98	18920	0.76	35	1998	0.620	●
Rolls-Royce	BR715-C1-30	4.6	32.15	21430	0.76	35	1998	0.620	●
Rolls-Royce	Trent 1000-A	9.5	41.00	70000	0.85	35	2007	0.506	●
Rolls-Royce	Trent 553-61	7.5	35.19	56620	0.82	35	2000	0.539	●

● $h \geq 0.50$ in.

SFW – Subsonic Fixed Wing project
ERA – Environmentally Responsible Aviation project
AATT – Advanced Air Transport Technology project

TABLE IX.—Concluded.

Org.	Engine Model	BPR (SLS)	OPR (SLS)	Thrust, lbs (SLS)	Cruise Mach	Cruise Alt. k ft.	Year certified	Cruise TSFC lb/lbf.hr	Core Size
Rolls-Royce	Trent 556-61	7.5	36.70	56620	0.82	35	2000	0.539	●
Rolls-Royce	Trent 7000-72	9.0	45.40	73700	0.85	35	2018	0.506	●
Rolls-Royce	Trent 768	5.2	34.00	68400	0.82	35	1994	0.565	●
Rolls-Royce	Trent 772	5.0	35.80	71100	0.82	35	1994	0.565	●
Rolls-Royce	Trent 772B-60	4.9	36.80	72000	0.82	35	1998	0.565	●
Rolls-Royce	Trent 875	6.1	35.42	79100	0.83	35	1995	0.560	●
Rolls-Royce	Trent 877	6.0	36.30	81300	0.83	35	1995	0.560	●
Rolls-Royce	Trent 884	5.9	38.96	87700	0.83	35	1995	0.560	●
Rolls-Royce	Trent 890-17	6.2	40.70	91300	0.83	35	1995	0.560	●
Rolls-Royce	Trent 892	5.7	41.38	92500	0.83	35	1997	0.560	●
Rolls-Royce	Trent 895	5.7	41.52	92900	0.83	35	1999	0.560	●
Rolls-Royce	Trent 970-84	8.5	38.00	76100	0.85	35	2006	0.518	●
Rolls-Royce	Trent XWB-84	9.0	41.10	85200	0.85	35	2013	0.488	●
Rolls Royce	Trent XWB-97	8.0	48.60	98200	0.85	35	2017	0.488	●
IAE	V2500-A1	5.3	29.80	25000	0.80	35	1988	0.580	●
IAE	V2522-A5	4.9	25.70	23043	0.80	35	1996	0.575	●
IAE	V2524-A5	4.8	26.90	24518	0.80	35	1996	0.575	●
IAE	V2525-D5	4.8	27.20	25000	0.80	35	1992	0.575	●
IAE	V2527-A5	4.8	27.20	25000	0.80	35	1992	0.575	●
IAE	V2528-D5	4.7	30.00	28000	0.80	35	1992	0.575	●
IAE	V2530-A5	4.6	32.00	29900	0.80	35	1992	0.575	●
IAE	V2533-A5	4.5	33.44	31600	0.80	35	1996	0.575	●
NASA SFW	UHB	18.8	44.7	36833	0.80	35	2015	0.477	●
NASA AATT	N3CC-2016	17.6	31.6	18830	0.70	35	2040	0.461	▲
NASA AATT	N3CC-2017	17.3	36.9	21515	0.78	35	2040	0.485	▲
NASA AATT	N+3	27.5	36.6	28620	0.80	35	2040	0.464	▲
NASA AATT	Small Core geared	25.5	38.8	37659	0.80	35	2040	0.460	▲
NASA AATT	N3CC-2018	21.6	36.7	21662	0.79	37.7	2040	0.479	▲
NASA ERA	Large-DD-2015	16.6	43.7	71792	0.80	35	2030	0.480	●
NASA ERA	Large-DD-2015-HWB-V1	14.4	48.9	67183	0.80	35	2030	0.485	●
NASA ERA	Large-DD-2015-HWB-V2	13.7	49.8	67233	0.80	35	2030	0.487	●
NASA ERA	Large-Geared-2015-HWB-V3	20.0	47.2	56172	0.80	35	2030	0.465	▲
NASA ERA	Large-Geared-2015-HWB-V2	20.0	47.1	67423	0.80	35	2030	0.464	●
NASA ERA	Large-Geared-2015-HWB	19.3	47.2	67386	0.80	35	2030	0.466	●
NASA ERA	Large-Geared-2015	24.7	39.9	74149	0.80	35	2030	0.458	●
NASA ERA	Medium-Geared-2015	23.9	38.4	45829	0.80	35	2030	0.466	●
NASA ERA	Medium-Geared-2015-V2	24.8	38.5	45799	0.80	35	2030	0.465	●
NASA ERA	Small-DD-2015	9.9	28.7	14647	0.80	35	2030	0.526	▲
NASA ERA	Small-DD-2015-V2	10.0	28.7	14686	0.80	35	2030	0.525	▲
NASA ERA	Small-Geared-2015	27.0	24.6	21525	0.80	35	2030	0.485	▲
NASA ERA	Small-Geared-2015-V2	27.4	24.8	21553	0.80	35	2030	0.483	▲
NASA ERA	Large-DD-2014	16.2	47.4	80071	0.80	35	2030	0.469	●
NASA ERA	Large-Geared-2014	22.4	47.2	87496	0.80	35	2030	0.458	●
NASA ERA	Medium-Geared-2014	22.4	44.7	51295	0.80	35	2030	0.467	●
NASA ERA	Small-DD-2014	9.8	29.7	15566	0.80	35	2030	0.519	▲
NASA ERA	Small-Geared-2014	24.7	29.2	24887	0.80	35	2030	0.486	▲
NASA SFW	SA-FPR1.4-DD-2D	18.4	33.1	23813	0.80	35	2025	0.479	▲
NASA SFW	SA-FPR1.5-DD-2D	15.0	33.8	23370	0.80	35	2025	0.496	▲
NASA SFW	SA-FPR1.6-DD-2D	12.7	34.4	23046	0.80	35	2025	0.510	▲
NASA SFW	SA-FPR1.7-DD-2D	10.9	35	22734	0.80	35	2025	0.525	▲
NASA SFW	SA-FPR1.3-GR-HW-2D	24.1	32.6	26343	0.80	35	2025	0.470	▲
NASA SFW	SA-FPR1.4-GR-HW-2D	17.5	33.8	24917	0.80	35	2025	0.486	▲
NASA SFW	SA-FPR1.5-GR-HW-2D	14.6	33.5	23369	0.80	35	2025	0.502	▲
NASA SFW	SA-FPR1.6-GR-HW-2D	12.4	34	22924	0.80	35	2025	0.517	▲
NASA SFW	SA-FPR1.3-GR-HW-2E	26.0	32.3	28358	0.80	35	2025	0.473	▲
NASA SFW	SA-FPR1.4-GR-HW-2E	18.0	33.8	26575	0.80	35	2025	0.495	▲
NASA SFW	SA-FPR1.5-GR-HW-2E	12.1	35.4	24686	0.80	35	2025	0.515	▲
NASA SFW	SA-FPR1.6-GR-HW-2E	9.9	36.3	24262	0.80	35	2025	0.534	▲
NASA SFW	SA-FPR1.7-DD-LW-2E	8.5	37.6	23889	0.80	35	2025	0.547	●
NASA SFW	Simulated Genx	9.2	41.4	63800	0.85	35	2008	0.523	●
NASA SFW	Simulated GE90-110B	7.2	42	110000	0.85	35	2003	0.549	●

● $h \geq 0.50$ in. ▲ $h < 0.50$ in.

SFW – Subsonic Fixed Wing project
ERA – Environmentally Responsible Aviation project
AATT – Advanced Air Transport Technology project